NEW CRYSTAL BARREL RESULTS IN THE SCALAR MESON SECTOR

Curtis A. Meyer
Carnegie Mellon University, Pittsburgh, PA 15213

The Crystal Barrel Collaboration*

ABSTRACT

Recent observations by the Crystal Barrel experiment of two scalar resonances, $f_0(1365)$ and $a_0(1450)$ have allowed us to clarify the members of the scalar nonet. These states replace the $f_0(950)$ and $a_0(980)$. In addition, a third scalar, $f_0(1500)$, appears to be supernumerary and its apparent flavor–blind decays make it a good candidate for the scalar glueball expected near 1500 MeV. However, this interpretation still awaits analysis of its $\bar{K}K$ decays.

1. The Crystal Barrel Detector

The Crystal Barrel detector, (Fig. 1), at LEAR [1] is a nearly 4π apparatus for detecting both charged particles and photons and is used to study $\bar{p}p$ annihilation at rest and in flight up to 1.9GeV/c. Antiprotons enter along the axis of the 1.5 T solenoidal field, and stop in a liquid hydrogen target. They annihilate, and the resulting $\pi^{\pm}$, $K^{\pm}$ and γ's are tracked outward through the detector. Immediately outside the hydrogen target are two cylindrical multiwire proportional chambers, PWC used to either trigger on or veto events with charged particles. Next is a 23 layer cylindrical drift chamber, (JDC). The chamber is divided axially into 30 sectors, with an 8mm wire spacing between adjacent radial layers. The wires are read out at each end to provide a z–measurement through charge division. Outside the JDC is the CsI(Tl) barrel built with 1380 16 radiation length crystals. The crystals are arranged in a center–pointing geometry, and the calorimeter has achieved an energy resolution of 2.5% at 1GeV.

2. The Data Analysis

The data discussed in this paper come from 3.8×10^6 minimum–bias triggers, and 16.8×10^6 all-neutral triggers taken at rest on a liquid hydrogen target. The minimum–bias trigger requires only that a $\bar{p}$ enter the target and annihilate. In addition to the

*C. Amsler, V. V. Anisovich, D. S. Armstrong, I. Augustin, C.A. Baker, B. Barnett, C.J. Batty, K. Beuchert, P. Birien, P. Blüm, R. Bossingham, K. Braune, J. Brose, D.V. Bugg, M. Burchell, T. Case, A. Cooper, K.M. Crowe, T. Degener, H. P. Dietz, S. v. Dombrowski, M. Doser, W. Dünnweber, D. Engelhardt, M. Englert, M. Faessler, C. Felix, R. Hackmann, R. Haddock, F. Heinsius, M. Herz, N. P. Hessey, P. Hidas, P. Illinger, D. Jamnik, H. Kalinowsky, B. Kämmle, T. Kiel, J. Kisiel, E. Klempt, M. Kobel, H. Koch, C. Kolo, K. Königsmann, M. Kunze, R. Landua, F. Loser, J. Lüdemann, H. Matthaey, M. Merkel, J. P. Merlo, C.A. Meyer, L. Montanet, A. Noble, F. Ould–Saada, K. Peters, C. N. Pinder, G. Pinter, S. Ravndal, J. Salk, A. V. Sarantsev, E. Schäfer, P. Schmidt, S. Spanier, C. Straßburger, U. Strohbusch, M. Suffert, D. Urner, C. Völcker, F. Walter, D. Walther, U. Wiedner, N. Winter, J. Zoll, B. S. Zou, and Č. Zupančič

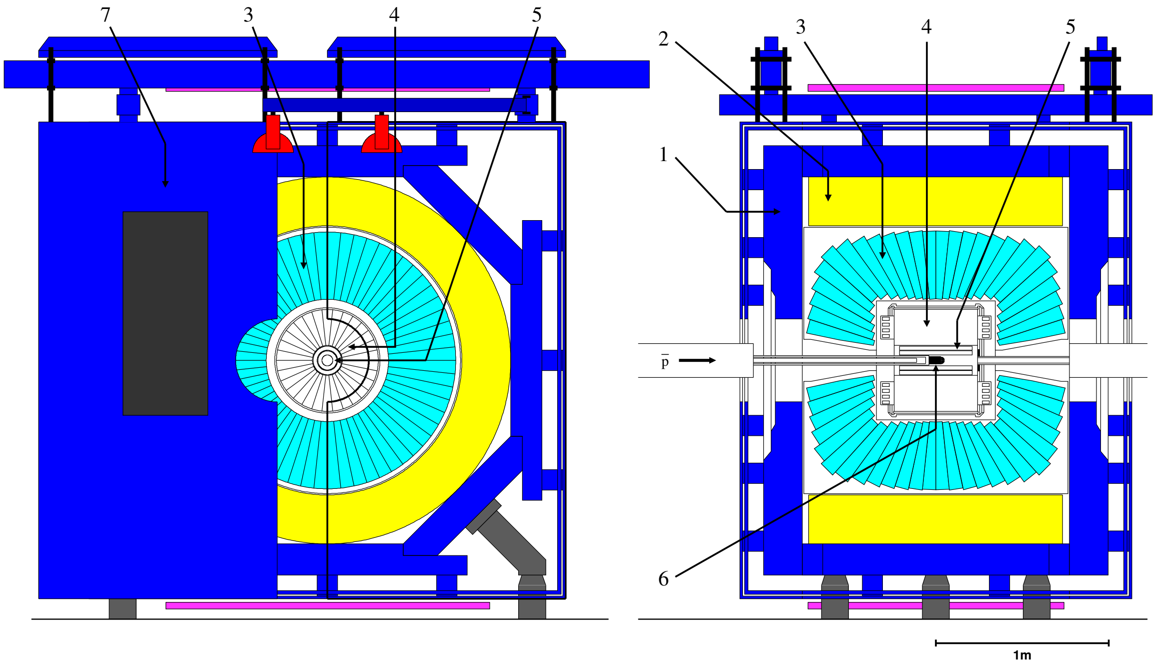

Figure 1: The Crystal Barrel detector. Magnet yoke (1), magnet coils (2), CsI–calorimeter (3), JDC (4), PWC (5), target (6), one half of the end plate (7).

minimum–bias trigger, the all-neutral trigger requires that no charged particles are observed in the PWC. $\bar{p}p \rightarrow$ *all netral* represents about 4% of all annihilations at rest, so the 16.8×10^6 all–neutral triggers represents approximately 420×10^6 minimum bias events.

The all–neutral data have been reconstructed and those events consistent with $\bar{p}p \rightarrow 6\gamma$ have been selected. These events have then been kinematically fit to several three pseudoscalar hypothesises, ($\pi^\circ \rightarrow \gamma\gamma$, $\eta \rightarrow \gamma\gamma$ and $\eta' \rightarrow \gamma\gamma$). These fits yield 712k $\bar{p}p \rightarrow \pi^\circ\pi^\circ\pi^\circ$, 280k $\bar{p}p \rightarrow \eta\pi^\circ\pi^\circ$, 31k $\bar{p}p \rightarrow \eta\eta\pi^\circ$ and 130 $\bar{p}p \rightarrow \eta'\eta\pi^\circ$ events which are used as input to the spin–parity analysis. The spin–parity analysis has been performed using two different formalisms. In the first, the P–vector approach [2] is used to represent the production amplitudes, and assumes complete factorization between production and the two–body final state interaction. In addition, the third particle is treated as a spectator. The second approach uses the "N/D" method [3, 4] which introduces an a priory unknown function $N(s)$ in the $\pi\pi$ S–wave. This second method is simultaneously applied to $\pi^\circ\pi^\circ\pi^\circ$, $\eta\pi^\circ\pi^\circ$ and $\eta\eta\pi^\circ$. In both approaches, the total transition amplitude from an initial state with quantum numbers J^{PC} to the final state is given as a sum over all possible two–body subsystems with all allowed relative angular momenta. In addition, a two–channel approach for the $\pi\pi$ S–wave with $\pi\pi$ as channel 1 and $K\bar{K}$ as channel 2 has been used. This is written in terms of a 2×2 K–matrix.

The $\bar{p}p \rightarrow \pi^\circ\pi^\circ\pi^\circ$ Dalitz plot (Fig. 2–left) shows several clear structures, seen simul-

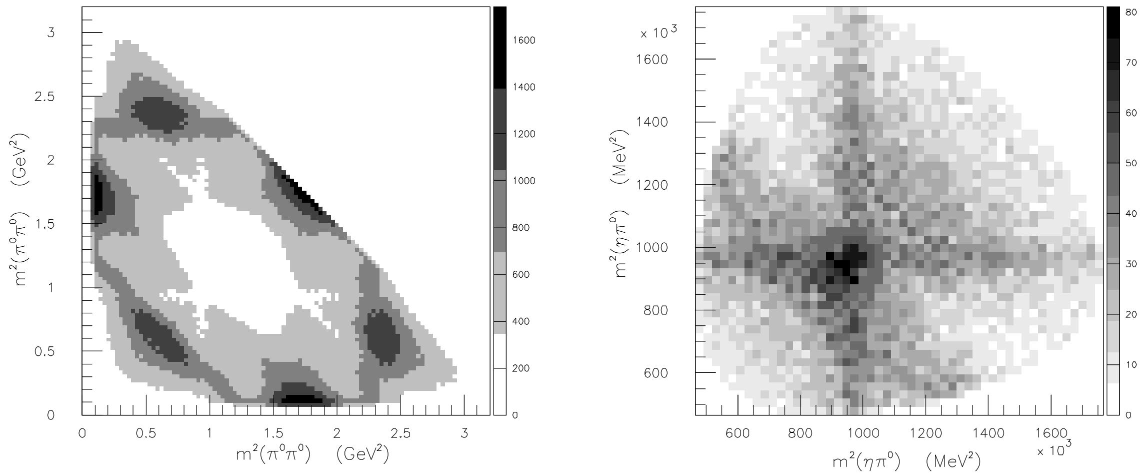

Figure 2: The Dalitz plots for $\bar{p}p \to \pi^\circ\pi^\circ\pi^\circ$ (left) and $\pi^\circ\eta\eta$ (right). The $f_0(1500)$ is seen clearly as the band near 1.25 GeV^2 in the $3\pi^\circ$ Dalitz plot. It is also seen as the lower diagonal band in the $\pi^\circ\eta\eta$ Dalitz plot.

taneously as three bands, vertical, horizontal and diagonal. The band near 0.9 GeV^2 corresponds to the $f_0(975)$, the two blobs at the upper and lower edge of the plot near 1.7 GeV^2 corresponds to the $f_2(1270)$, and the vertical band near 2.25 GeV^2 corresponds to a new scalar resonance, the $f_0(1500)$. The blob near 2.4 GeV^2 is caused by interference between the low–mass $\pi\pi$ system, and a tensor state, ($J^{PC} = 2^{++}$) near 1550 MeV. In addition, the fit to this Dalitz plot requires a broad, inelastic scalar state at a mass of 1365 MeV, which is probably the $f_0(1400)$ and inclusion of the low mass $\pi\pi$ S–wave as given by Au *et al.* [5].

In the $\eta\eta\pi^\circ$ Dalitz plot, (Fig. 2–right), resonances in the $\eta\pi^\circ$ system are seen as horizontal and vertical bands, while resonances in the $\eta\eta$ system are seen as diagonal bands. The horizontal and vertical crossing bands near $950 \cdot 10^3$ MeV^2 show a clear signal for the $a_0(980) \to \eta\pi^\circ$. In addition, there are two diagonal bands corresponding to the $f_0(1365) \to \eta\eta$ and the $f_0(1500) \to \eta\eta$. In addition, the fit requires the low mass $\pi\pi$ S–wave, and a small contribution from a tensor state at 1520 [6]. A simultaneous spin–parity analysis [4] to a subset of both $\pi^\circ\pi^\circ\pi^\circ$ and $\eta\eta\pi^\circ$ yields the following parameters for the two isoscalar scalar resonances.

$$\begin{array}{lll} f_0(1365) & m = 1365^{+20}_{-55} & \Gamma = 267 \pm 70 \\ f_0(1500) & m = 1520 \pm 25 & \Gamma = 148^{+20}_{-25} \end{array}$$

An analysis using the full statistics pulls the mass of the 1520 state down to about 1500.

The Dalitz plot for $\bar{p}p \to \eta\pi^\circ\pi^\circ$ (Fig. 3–left), exhibits a very complicated interference pattern which is evidence for dominance of a single initial state. This is confirmed by a spin–parity analysis [7] of these data coupled to $\pi^\circ\pi^\circ\pi^\circ$ and $\eta\eta\pi^\circ$. The $\eta\pi^\circ\pi^\circ$ final state arises almost entirely from the $^1S_0$ state of the $\bar{p}p$ atom. The analysis

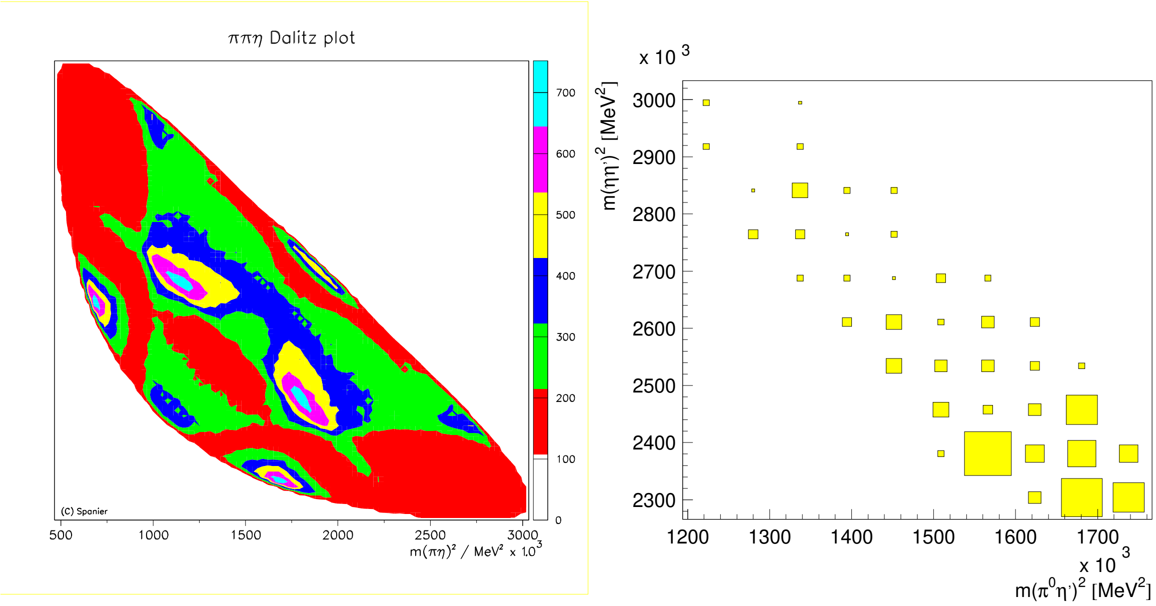

Figure 3: The Dalitz plots for $\bar{p}p \to \pi^\circ\pi^\circ\eta$ (left) and $\eta'\eta\pi^\circ$ (right).

explains the data using the following amplitudes. [$\pi\pi$ S–wave] Including the AMP parametrization [5], $f_0(975)$ and $f_0(1365)$ explain 50 to 55% of the data. [$\pi\eta$ S–wave] The $a_0(980)$ explains 13 to 15% of the data. In addition the data demand a second resonance, the $a_0(1450)$ which explains 5% of the data. Ignoring the second resonance causes the χ^2/N_{dof} to increase from 1.2 to 2.5. [$\pi\eta$ P–wave] A broad non–resonant background wave is needed to explain about 1.5 to 4.5% of the data. We exclude a resonance interpretation with the mass and width reported by GAMS for the $\hat{\rho}(1405)$ [8]. [$\eta\pi$ D–wave] The $a_2(1320)$ describes 18 to 28% of the data. In addition, a second a_2 is needed to account for about 2% of the data. However, its mass is at the edge of phase space, and we do not claim that this is a resonance.

The Dalitz plot for $\bar{p}p \to \eta'\eta\pi^\circ$ is shown in Fig. 3–right. Of the 158 events in this plot, 28 are estimated to be from background distributed uniformly over the plot. The enhancement in the lower right corner of the plot is most likely a structure in the $\eta'\eta$ system. A spin parity analysis is currently under way to determine if this is the $f_0(1500) \to \eta'\eta$.

The 3.8×10^6 minimum–bias events have been reconstructed, and kinematically fit to the hypothesis $\bar{p}p \to \pi^+\pi^-\pi^\circ\pi^\circ\pi^\circ$. The 38k events which satisfy this hypothesis have then been examined to search for resonances decaying into $\rho^+\rho^-$ [9]. The analysis of these data show the presence of a scalar resonance X decaying into $\rho\rho$ and $\sigma\sigma$, where σ is the $\pi\pi$ s–wave as given by the AMP parametrization [5]. We find $m_X = 1374 \pm 38$ MeV and $\Gamma_X = 375 \pm 61$ MeV. Under the assumption that this is isoscalar, it is probably the inelastic $f_0(1365)$ seen above, and we find:

$$
\begin{aligned}
BR[\bar{p}p \to f_0(1365)\pi^\circ \to \rho\rho\pi^\circ] &= (30.6 \pm 3.9) \cdot 10^{-3} \\
BR[\bar{p}p \to f_0(1365)\pi^\circ \to \sigma\sigma\pi^\circ] &= (19 \pm 2) \cdot 10^{-3}.
\end{aligned}
$$

3. New Results in the Scalar Meson Sector

3.1. The $f_0(1365)$

The Crystal Barrel has observed the $f_0(1365)$ decaying into $\pi\pi$, $\eta\eta$ and 4π. The $\pi\pi$ and $\eta\eta$ analysis indicate that the $f_0(1365)$ is an inelastic object, which is confirmed by our large decay into 4π. This object is likely to be the $f_0(1400)$, however our large 4π decay is in disagreement with the well known $f_0(1400)$, which decays 93% of the time into $\pi\pi$. We estimate that the $\eta\eta$:$\pi\pi$:4π are 1:5:$\leq$25. The $f_0(1365)$ is probably the mostly $u\bar{u}+d\bar{d}$ isoscalar member of the scalar nonet, replacing the $f_0(975)$ of the Particle Data Group [10].

3.2. The $a_0(1450)$

The $a_0(1450)$ has been observed to decay into $\eta\pi^{\circ}$ where we find $m = (1450{\pm}40)MeV$ and $\Gamma = (270 \pm 40)MeV$. An $a_0(1320)$ with a width of 130 MeV has been reported in the $\eta\pi$ system produced in $\pi^- p \rightarrow \pi^- \eta p$ [8]. Our data exclude this mass and width for the $a_0(1450)$. The mass and width make the $a_0(1450)$ the natural candidate for the isovector scalar meson, replacing the $a_0(980)$ of the Particle Data Group [10].

3.3. The $f_0(1500)$

Crystal Barrel observes the $f_0(1500)$ decaying into $\pi\pi$ and $\eta\eta$. In addition, a threshold enhancement in the $\eta\eta'$ invariant mass may also be the $f_0(1500)$. So what is this resonance? It would be natural to try and assign it as the mostly $s\bar{s}$ isoscalar member of the scalar nonet. However, if this were correct one would expect the dominant decay to be $K\bar{K}$. The decays of the $f_2'(1525)$ could guide us here: $K\bar{K}$ 71%, $\eta\eta$ 28% and $\pi\pi$ 1%. Assuming 10% $\pi\pi$ and 60% $K\bar{K}$, one would expect that $BR[\bar{p}p \rightarrow f_0(1500)\pi^{\circ} \rightarrow K^+K^-\pi^{\circ}]$ to be on order of 1% — Crystal Barrel observes no signal at such a level. The $f_0(1500)$ is most likely not a member of the scalar nonet.

Another state, the $f_0(1590)$ or G meson has been observed by GAMS in $\pi^- p \rightarrow Gn$ [11], and seen to decay into $\eta'\eta$, $\eta\eta$ and $4\pi^{\circ}$. Are the $f_0(1500)$ and the $f_0(1590)$ the same? GAMS finds that the $f_0(1590)$ decays most strongly to $\eta'\eta$, while Crystal Barrel places an upper limit of $\eta\eta$:$\eta'\eta$ of 4:1. At present, it seems unlikely that these are the same states. The LASS group has reported a scalar state, the $f_0(1520)$ [12] in the reaction $K^- p \rightarrow K^+K^-\Lambda$. However, given that this state is produced in a strangeness–rich environment, and decays to $K\bar{K}$, it seems unlikely that this is the same state as the $f_0(1500)$. This LASS state is however a good candidate for the remaining isoscalar member of the scalar nonet.

Lattice calculations predict that the lowest mass scalar glueball should have a mass around 1500 MeV. In addition, the decay modes for a glueball are expected to be flavor blind. If we assume that the enhancement seen in the $\eta'\eta$ invariant mass is indeed the $f_0(1500)$, then from the Crystal Barrel data one can extract the following production and decay ratios [13].

$$\begin{aligned} BR(\bar{p}p \to \pi^\circ f_0(1500), f_0(1500) \to \pi\pi) &= (38 \pm 10.0) \cdot 10^{-4} \\ BR(\bar{p}p \to \pi^\circ f_0(1500), f_0(1500) \to \eta\eta) &= (6.3 \pm 2.8) \cdot 10^{-4} \\ BR(\bar{p}p \to \pi^\circ f_0(1500), f_0(1500) \to \eta'\eta) &= (1.5 \pm 0.5) \cdot 10^{-4} \end{aligned}$$

These have been corrected for the 2γ decay modes, and the isospin of the π. In order to identify the $f_0(1500)$ as a scalar glueball, it will be necessary to see its $K\bar{K}$ decay. This is currently under investigation in $\bar{p}p \to K_L K_L \pi^\circ$. In addition, a special K_S trigger will be brought online at the end of '94 to study $\bar{p}p \to K_S K_S \pi^\circ$. Presently, we can use bubble chamber results for $\bar{p}p \to \pi^\circ K\bar{K}$ [14] to obtain an upper limit for $f_0(1500) \to K\bar{K}$. Correcting for the decay momentum of the $f_0(1500)$ then leads to the following decay pattern:

$$f_0(1500) \to \pi\pi : \eta\eta : \eta'\eta : K\bar{K} \quad = \quad 3 : (0.72 \pm 0.37) : (1.05 \pm 0.44) :< 0.40.$$

This is very suggestive of the flavor–blind decay of a glueball, but without information of the $K\bar{K}$ decay mode it is very difficult to confirm. In addition, the preliminary results still await the completion of the ongoing spin–partity analysis, and the planned collection of $K\bar{K}\pi$ data at the end of '94.

4. References

1. E. Aker *et al.*, **Nucl. Instrum. Methods A321**, 69, (1992).
2. S. U. Chung, *et al.*, submitted to **Z. Phys. C**, (1994).
3. D. V. Bugg, *et al.*, submitted to **Phys. Rev. D.**, (1994).
4. V. V. Anisovich, *et al.*, **Phys. Lett. B323**, 233, (1994).
5. K. L. Au, D. Morgan and M. R. Pennington, **Phys. Rev. D35**, 1633, (1987).
6. C. Amsler *et al.*, **Phys. Lett. B291**, 347, (1992).
7. C. Amsler, *et al.*, Submitted to **Phys. Lett. B**, (1994).
8. M. Boutemeur and M. Poulet, Hadron 89, ed. F. Binon, J. M. Frère, J. P. Peigneux – (Ed. Frontiérs 1989), p.119.
9. C. Amsler, *et al.*, **Phys. Lett. B322**, 431, (1994).
10. K. Hikasa, *et al.*, **Phys. Rev. D45 II**, (1992).
11. F. Binon *et al.*, **Nuovo Cimento 78A**, 313, (1983), and **80A**, 303, (1984).
12. D. Aston *et al.*, **Nucl. Phys. B301**, 525, (1988).
13. R. Hackmann, Proceedings of the Recontre de Moriond, (1994).
14. L. Gray *et al.*, **Phys. Rev. D27**, 307, (1983).